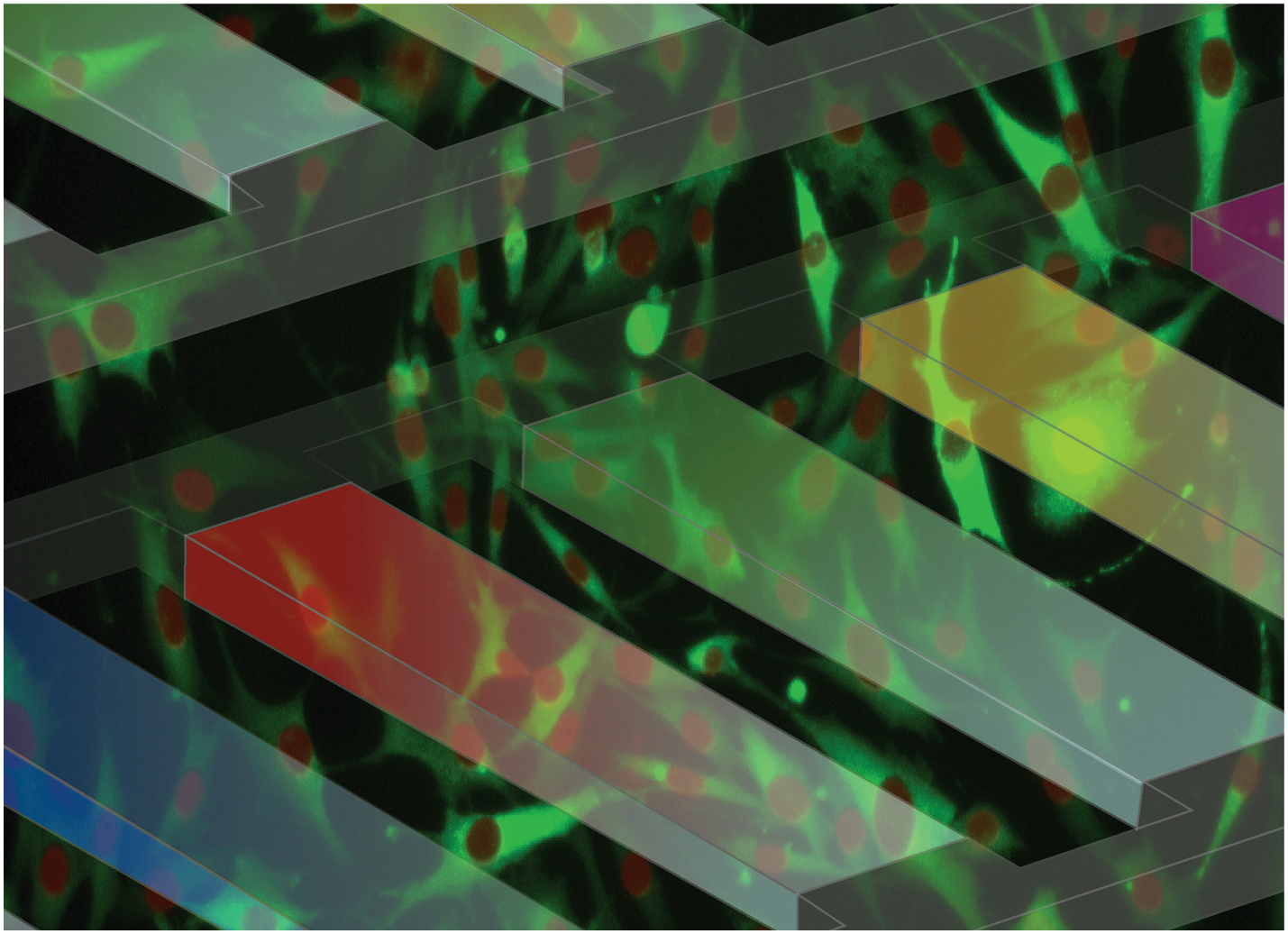

Featuring work from the group of Savaş Tay at the Department of Biosystems Science and Engineering, ETH Zurich, in Basel, Switzerland.

Title: Flow-switching allows independently programmable, extremely stable, high-throughput diffusion-based gradients

An automated microfluidic cell culture platform that maintains independently programmable diffusion-based gradients is reported.

As featured in:

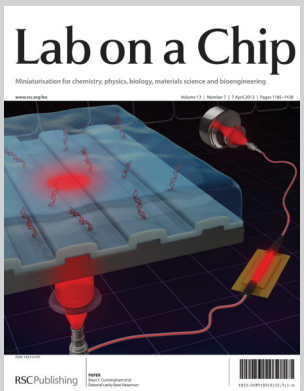

See Tino Frank and Savaş Tay., *Lab Chip*, 2013, **13**, 1273.

RSC Publishing

www.rsc.org/loc

Registered Charity Number 207890

Lab on a Chip

RSC Publishing

PAPER

View Article Online
View Journal | View Issue

Cite this: *Lab Chip*, 2013, **13**, 1273

Flow-switching allows independently programmable, extremely stable, high-throughput diffusion-based gradients†

Tino Frank and Savaş Tay*

Received 23rd September 2012,
Accepted 17th January 2013

DOI: 10.1039/c3lc41076e

www.rsc.org/loc

An automated microfluidic cell culture platform that creates and maintains independently programmable diffusion-based gradients is reported. Temporal modulation of the source and sink flow patterns allow generation of extremely stable spatial gradients. We developed a system that integrates 30 parallel gradients in a single device, with 10 different chemical formulations and 3 replicates. Mammalian fibroblast and macrophage cells were screened for NFκB pathway activity under gradients of TNFα, PDGF, and LPS, and multiparameter measurements were performed to demonstrate the capability of the device in dynamic single-cell analysis.

Introduction

Cells often rely on spatiotemporal gradients of secreted proteins to transmit signals.[1] Leukocytes, for example, find their invasion site by signals mediated by a chemokine gradient.[2] An armada of morphogen gradients patterns the drosophila larva,[3] and synapse formation is guided by gradient signalling.[4] Yeast finds its budding partner by a pheromone gradient[5] and even human life starts by gradient-guided sperms finding the ovum.[6] It is thus desirable to create stable chemical gradients in a laboratory setting to study and even recapitulate these processes *in vitro*.

One of the simplest ways to generate a gradient is to utilize parallel laminar-flow patterns containing different concentrations of proteins of interest.[6–8] This method is especially efficient in rapidly establishing or changing the gradient profile. However, the viability of many cell types as well as the integrity of certain cellular processes are compromised under continuous flow.[9] Besides, flow based systems are not suited to study non-adhering cell types that will simply wash out of the field of view. Most importantly, secreted signalling molecules such as cytokines and chemokines are removed by continuous flow (Fig. 1A), preventing the study of inter-cellular signalling events mediated by these factors.[10–12] This becomes a particularly severe limitation in the study of immune regulation, morphogenesis, or collective cell migration, processes that depend on cells establishing and responding to local spatiotemporal gradients.

Many signalling events in biological systems depend on diffusion-based signal propagation. Cells constantly secrete signalling molecules that diffuse in the extracellular environment and establish dynamic gradients, and nearby cells detect and interpret the local concentration in the gradient.[13] Biological pathways utilize surface receptors and network motifs to detect and process extracellular concentrations, which allow them to mount appropriate responses by modulating gene expression programs and cell behaviour. A prime example of such a signalling pathway is the NFκB, which generates digital and analogue outputs depending on the extracellular concentration of the signalling molecules such as TNFα.[14] Microfluidic diffusion-based gradient systems could significantly improve the study of cell signalling *in vitro*.

A simple rectangular source–sink configuration provides a linear, diffusion-based gradient across a microfluidic chamber (Fig. 2B). The source and the sink should be continuously replenished to maintain a constant gradient profile. This presents a technical difficulty: the pressure difference between the source and the sink should be set to an absolute minimum to prevent flow through the diffusion chamber (Supplementary Fig. 1†). Several strategies have been used to minimize this unwanted cross flow, such as increasing the fluidic resistance across the gradient chamber using very small grids of pillars,[15,16] or decreasing the fluidic resistance of the flow channels by making them significantly wider and taller than the cell culture area,[17,18] or using a physical barrier like a hydrogel layer that allows diffusion yet blocks flow,[19] or introducing semi-permeable membranes between flow and diffusion regions.[9,20] Although capable of creating stable gradients, these approaches require additional steps beyond standard soft-lithography that limit their scalability, flexibility and automation.

ETH Zurich, Department of Biosystems Science and Engineering, Mattenstrasse 26, 4058 Basel, Switzerland. E-mail: savas.tay@bsse.ethz.ch; Tel: +41 61 387 31 57

† Electronic supplementary information (ESI) available. See DOI: 10.1039/c3lc41076e

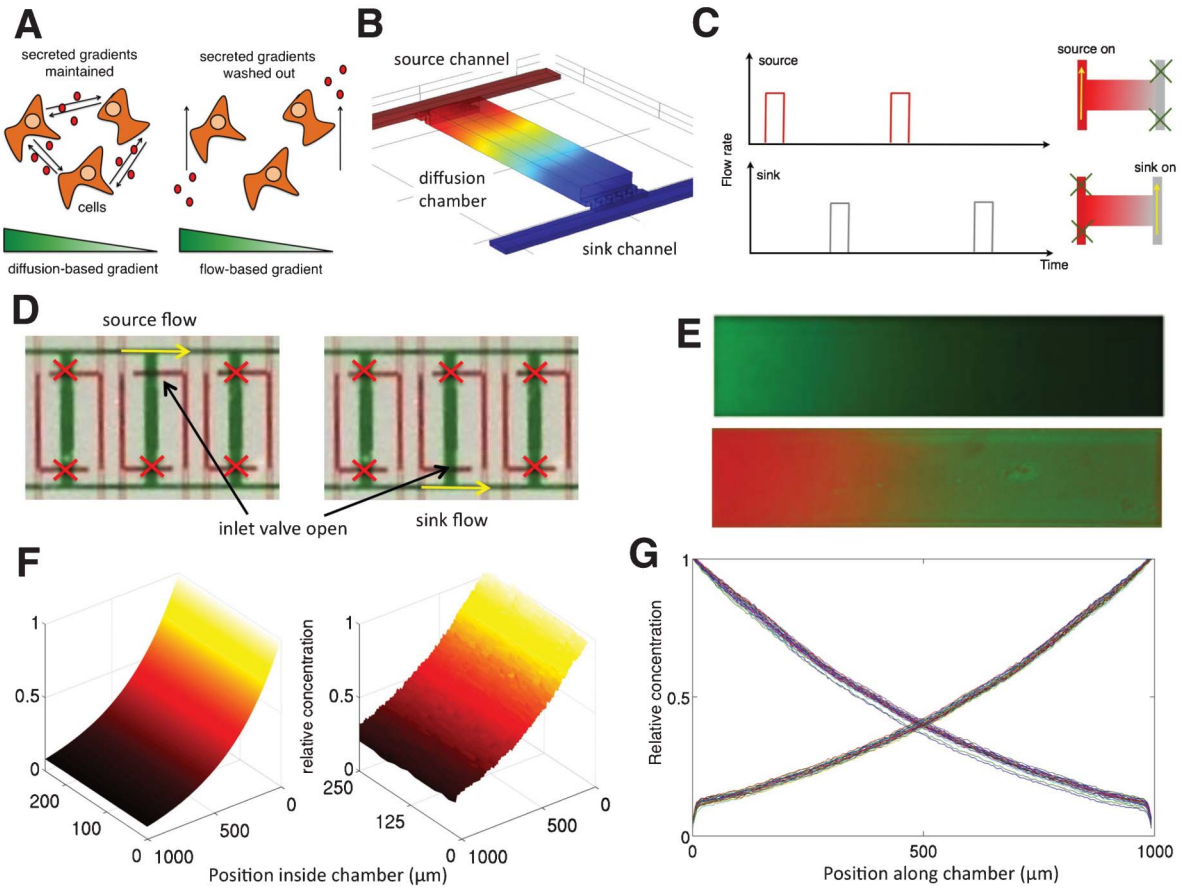

Fig. 1 (A) Comparison of cell signalling in diffusion-based and flow-based external gradients. Diffusion-based systems preserve cell-secreted gradients and allow cells to communicate with each other. Cell-secreted factors are washed away in flow-based gradients. (B) Simulation of the parallel source–sink geometry. Source channel is flowed with medium containing a protein (D = 100 μm^2 s^{-1}), and the sink channel carries cell culture media. The colours indicate the relative concentration (red: high, blue: low). A linear gradient across the diffusion chamber can be created by constantly flowing the source and sink channels, however small pressure variations between source and sink lead to cross-chamber flow (see Supplementary Fig. 1†). (C) Description of flow-switching for gradient formation. The source channel flows for 1 s every 2 min. The sink has the same frequency of flow, but shifted by 1 min. This scheme creates an efficient source–sink pair while preventing cross-flow, resulting in stable gradients. (D) Inlet valves seal the diffusion chamber during gradient maintenance. Red crosses indicate closed inlet valves. (E) Actual picture of a FITC–Dextran gradient over the diffusion chamber is shown (top). Picture of a two-sided opposing gradient using green FITC–Dextran in the sink and red Rhodamin–Dextran in the source is also shown (bottom). (F) The 2D spatial concentration profile of the green gradient shown in (E) is plotted on the right side. On the left, a COMSOL simulation of the measured gradient is plotted. (G) The concentration profile of the two-sided gradient in (E) is measured over 14 h, by taking pictures every 30 min (each measurement is shown with a different coloured line). The gradient shows excellent stability at all points inside the chamber. The curves with high concentration on the left hand side shows the Rhodamin–Dextran profile, where as the curves with maxima at the right hand side show the measurements of the FITC–Dextran.

Here we report a novel strategy to create diffusion-based microfluidic gradients that utilizes temporally modulated source and sink flow patterns (Fig. 1C and D), which eliminates the need for maximizing the fluidic resistance of the culture chambers. Only one side of the chamber is exposed to parallel flow at a time, resulting in a dead-end configuration, thereby eliminating cross-chamber flows. The switching is achieved through on-chip membrane valves (Fig. 1D) fabricated using standard multi-layer soft lithography. The valve-switching method provides a very simple geometry (a rectangular diffusion chamber connected to orthogonal source–sink channels, Fig. 1B) and therefore is easily scalable to higher throughput, with many gradients side-by-side in a single chip, using established integration methods.[21] We show that our method can create linear gradients that are extremely stable over night with less than 5% variation of the concentration at a given location (Fig. 1G). Furthermore, the flow-switching strategy allows many parallel and independently programmable chambers that each can encode a different gradient profile (Fig. 2). The type of protein, its average concentration and steepness (slope) of the gradient can easily be controlled in each diffusion chamber where cells are cultured, and can be changed over time if needed. Multiple proteins can be provided from the two sides of the diffusion chamber, creating opposing gradient profiles. Various adherent or non-adherent cells can be cultured and observed in virtually flow-free conditions (Fig. 3 and 4, and Supplementary Movies 1 and 2†).

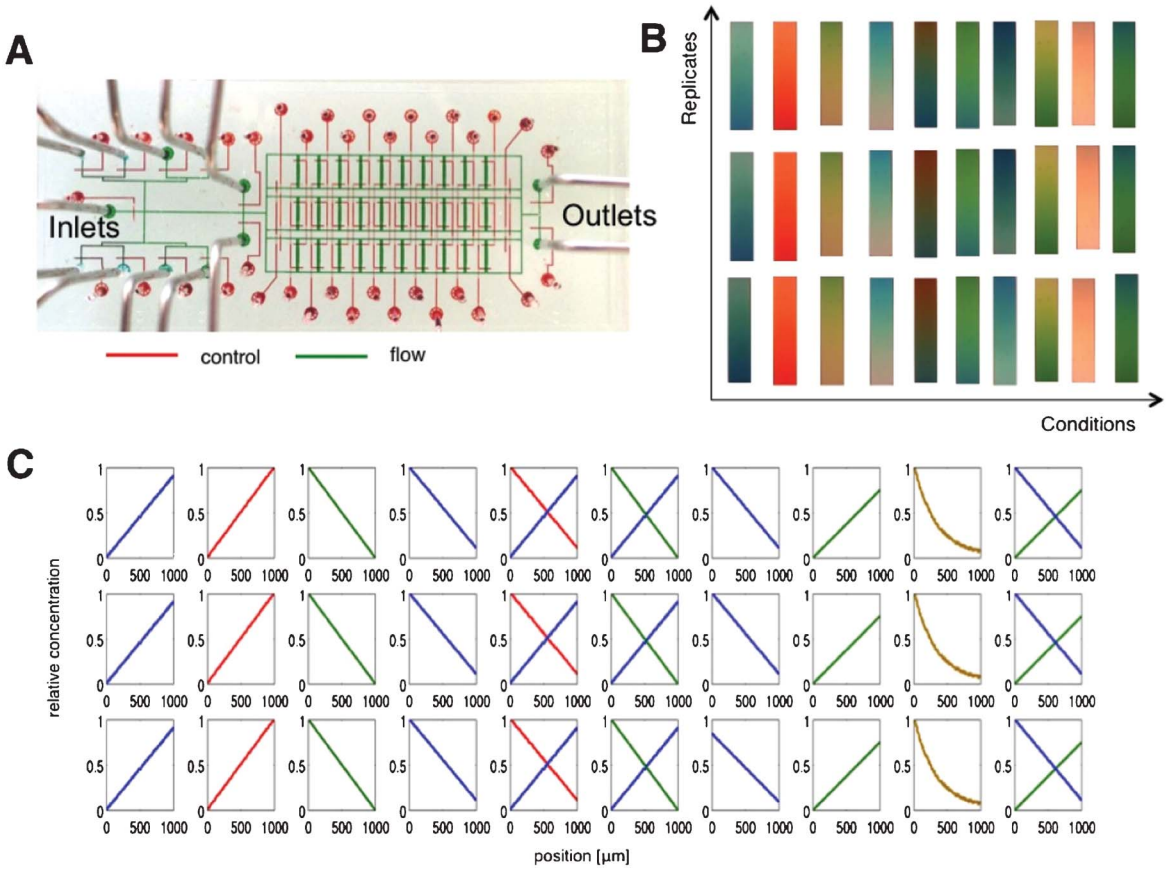

Fig. 2 (A) Picture of the 30-plex device. Flow and control channels are filled with green and red dye, respectively. On the left, the inputs for different medium compositions are placed in a manifold, followed by 30 independent gradient chambers, and at the very right the waste outlets are placed. The flow is from left to right. 10 rectangular diffusion chambers are put in series that allow the formulation of independent chemical conditions. Many such blocks of 10 chambers can be put in parallel and controlled simultaneously in order to maintain replicates (the current device has 3 such units). (B) Actual pictures of dye gradients simultaneously generated by the 30-plex chip are shown. Various food-dye and dextran concentrations are used to formulate different gradients in parallel in a single device. Different proteins, mean concentrations, gradient shapes and opposing gradients are possible. (C) Quantification of the gradients generated by the 30-plex device in a single experiment, showing the multiplexing capability of the device and excellent reproducibility between replicates.

Using this technique, we demonstrate a highly capable lab-on-chip device that can create 10 independently programmable chemical gradients with three replicates at once, with a total of 30 parallel cell culture chambers (Fig. 2). Each chamber can be treated with different surface coatings, and can be seeded with a different cell type. The simplicity of the gradient chamber design and the use of on-chip membrane valves allowed us to automate many processes such as surface treatments, cell seeding, cell feeding, generation of gradients, and retrieval of cells. The device was automated by custom software and was integrated into a fluorescence microscope, enabling a versatile cell culture system for studying cells at single-cell and population levels for long times with the ability to screen in parallel, independently programmable gradients. If needed, cells can be exposed to flow for quick feeding or clearing of gradients, or retrieval of cells for further analysis.

To demonstrate the feasibility of this system in cell signalling research, we perform cell-biological measurements on mammalian cells including 3T3 fibroblasts (Fig. 3 and Supplementary Movie 1†), and RAW macrophages (Fig. 4 and Supplementary Movie 2†). These cells are cultured in gradients of various signalling molecules such as *E. coli* lipopolysaccharide (LPS), tumour necrosis factor-α (TNF-α) and platelet-derived growth factor (PDGF), and their multi-parameter single-cell dynamic response characteristics are quantified using fluorescent fusion proteins. In particular, we focus on the single-cell dynamics of NFκB transcription factor p65, and observe the canonical response traits under various types of gradients through live-cell microscopy using our gradient system.

Methods and experiments

Chip fabrication

The design of the two-layer chip was implemented using standard multi-layer soft-lithography.[22] Briefly, the control layer was fabricated by spinning a 1 : 20 polydimethylsiloxane (PDMS) mixture to a height of 30 μm on an SU8 master mould. Pouring 69 g of a 1 : 5 PDMS mixture on an AZ-50XT reflowed

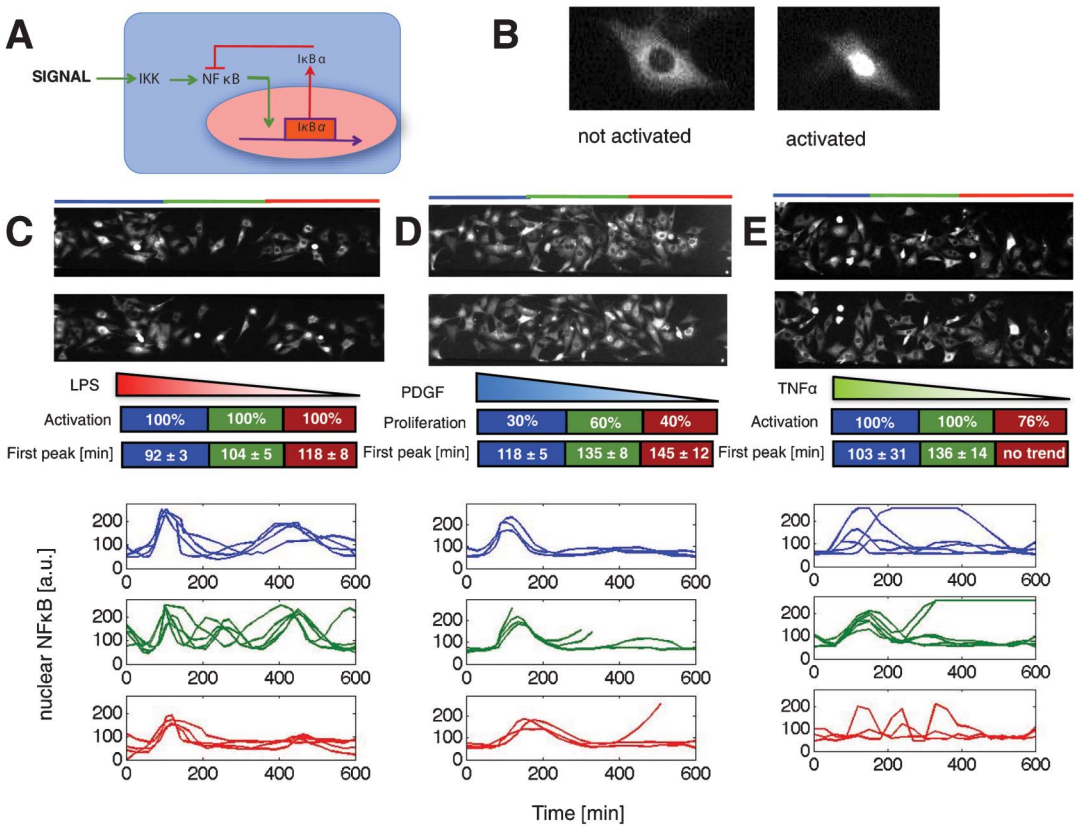

Fig. 3 Multiparameter analysis of 3T3 fibroblasts in spatial gradients of LPS, PDGF and TNFα. The cells were cultured in various gradients, and fluorescence images in green and red were taken every 5 min. Sample single-cell traces are shown. (A) Simplified signalling network of NFκB. Extracellular signals activate IKK that phosphorylates IkBα, and NFκB translocates into the nucleus. Newly synthesized IkBα binds to NFκB and moves it out of the nucleus. (B) Fluorescence picture of a resting and activated cell, showing accumulation of NFκB in the nucleus when stimulated. (C) Single-cell response to the LPS gradient. The pictures show cells at the time points t = 100 min (top) and 120 min (bottom). The blue color indicates the high concentration, green the middle range and red shows the low concentration range. The nuclear localization traces at the bottom show NFκB activity in single cells at different locations in the gradient, coded by their respective colour. (D) Single-cell response to the PDGF-BB gradient. Lines ending before T = 600 min indicate cell division. (E) Single-cell response to the TNFα gradient.

master mould created the flow layer. Both layers were hard baked for 1 h, and were bonded using oxygen-plasma treatment. After alignment and plasma bonding, the chips were cured for one week at 80 °C.

Chip operation and control

The control channels were connected *via* Tygon tubing to solenoid valves (Festo) and were controlled with a custom LabVIEW program, using the control box system by Gomez *et al.*[23] The valves were operated at a pressure of 1 bar.

Reagents and surface coating

The soluble reagents were dissolved to their dedicated maximal concentration in cell culture media and were serially diluted. *E. coli* derived LPS (Sigma-Aldrich) c_{max} = 1000 ng mL^{-1} was used. Recombinant mouse TNFα (Invitrogen) was used with c_{max} = 10 ng mL^{-1}. Recombinant rat PDGF-BB (Sigma-Aldrich) was used at 1 μM. The chips were coated with Fibronectin (c = 25 μg mL^{-1}, Millipore). The chip was flushed by the Fibronectin solution for 5 min and incubated overnight. It was then washed with cell culture media for 15 min and incubated for another hour before starting seeding cells. In order to avoid cells attaching in the channel in the multi-chamber device Pluronic (c = 10 μg mL^{-1}, Millipore) was incubated in the support channels for 1 h and washed with PBS for 30 min.

Generation of stable gradients using temporally modulated source–sink flow patterns

In order to create a chemical gradient across the diffusion chamber, membrane valves were used to direct the protein containing fluid to the source channel (Fig. 1C and D) for 5 s, resulting in charging the source channel with the new protein and completely clearing the previous one. Then, the inlet valve in front of the diffusion chamber is opened for 1 s, allowing the protein to diffuse inside. During this time, the sink inlet valve was kept closed to prevent cross-chamber flow (Fig. 1D). Thus, only one end of the diffusion chamber was open at a given time. The same procedure was repeated for the sink channel, resulting in removal of the proteins from the diffusion chamber. This temporally switched source–sink configuration (Fig. 1C) allowed us to generate extremely stable gradients across the diffusion chamber (Fig. 1E–G). Through simulations and experiments, we have seen that such temporal

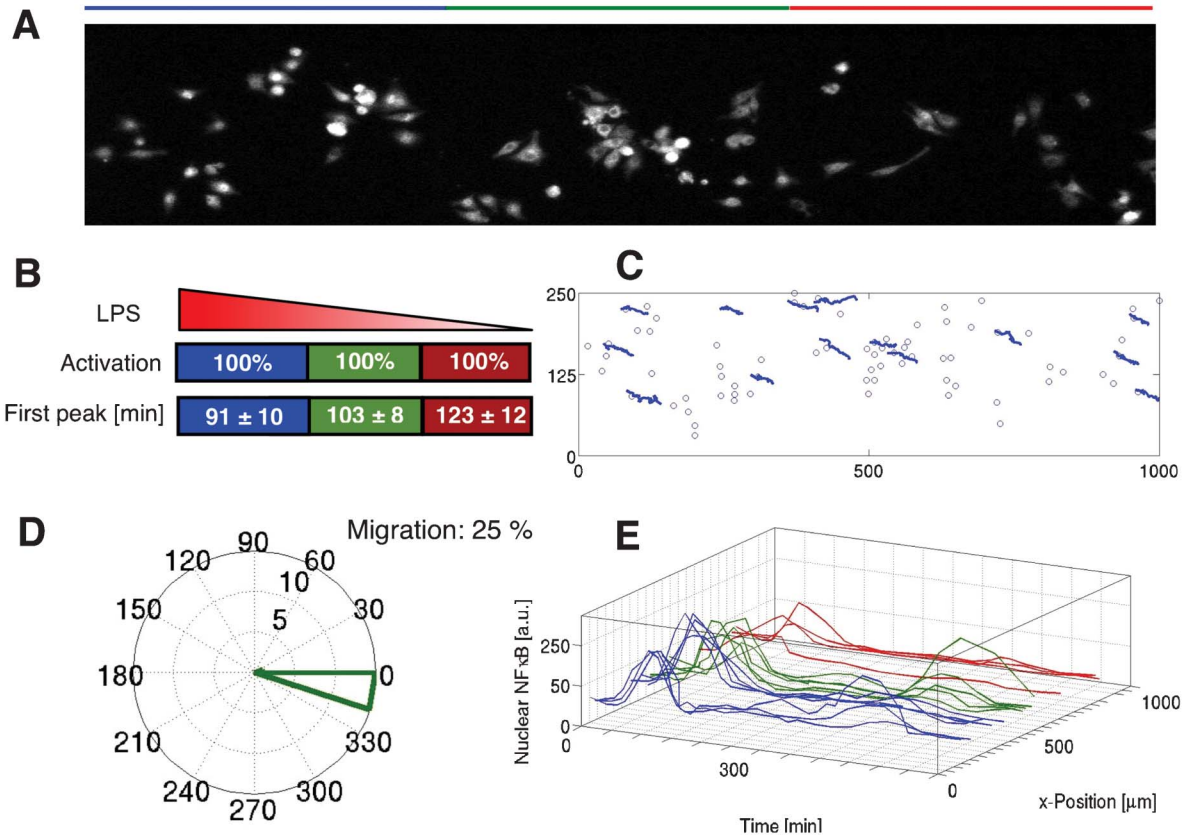

Fig. 4 Multiparameter analysis of RAW macrophages in an LPS gradient. (A) Fluorescence image of the diffusion chamber at t = 90 min after gradient initiation, showing a spatially variable response. Cells on the left (high LPS) have already activated NFκB at this time. (B) Temporal development of nuclear NFκB signalling. Ultimately, all cells activate but response time (first peak) is highly variable. Mean first peak times are given for three locations in the chamber. (C) Traces of moving cells. Nuclear positions are registered using a fluorescent protein fused to H2B. 25% of the cells move along the gradient (blue lines), while the rest are stationary (circles). (D) Orientation of cell migration. Cells move mostly along the gradient but in the opposite direction. (E) Spatio-temporal plot of the nuclear NFκB-intensities. The plots show traces of nuclear NFκB in single-cells according to their x-position and time.

modulation does not significantly affect the gradient profile as long as the switching time-scales involved are much smaller than the diffusion time of a typical protein. The calculated maximum error in concentration due to switching is 7% at any location in the diffusion chamber (Supplementary Fig. 6†), and it was experimentally measured to be 5% at the diffusion chambers (Fig. 1G). We found that we could pause up to 120 s between source and sink inputs without significantly affecting the gradient profile, allowing us to direct our attention to other on-chip diffusion chambers in the meantime. This way, the system generates as many as 10 parallel gradients along a single row where each could have a different protein, steepness and maximum concentration.

Gradient quantification

Gradients were quantified by using FITC–Dextran (Sigma-Aldrich) and Rhodamin–Dextran (Invitrogen) with a molecular weight of M = 40 000 g mol^{-1}, simulating a typical signalling protein. The devices were operated with a maintenance cycle of 2 min where any sink/source pair were opened for 1 s each (thus, each chamber is sealed for 118 s in each maintenance cycle). Pictures were taken every 30 min for 17 h. In order to determine the photobleaching, a chamber was fully filled with 300 μM of Rhodamin–Dextran and the decay of the signal was measured over 2 h (Supplementary Fig. 2†). The concentration–intensity relationship was calibrated by using a dilution row of 0 μM, 30 μM, 60 μM, 120 μM, 180 μM and 300 μM. Since the concentration only changes along the diffusion chamber length and is invariant in the direction of the supply channel, a horizontally averaged one dimensional concentration profile is reported. The signals were background corrected and normalized by the highest concentration from the source channel. All numerical processing were done in MATLAB.

Cell culture

Dissociated RAW macrophages and NIH 3T3 fibroblasts were seeded in the diffusion chambers and were allowed to settle for 1 h before each experiment. The NIH 3T3 ($p65^{-/-}$) fibroblasts containing H2B-GFP nuclear marker and p65-DsRed fusion protein[14] were cultured in a DMEM (Invitrogen) with FBS (10%, Sigma Aldrich), GlutaMax (1× Invitrogen), streptomycin (100 U mL^{-1}, Invitrogen) and penicillin (100 μg mL^{-1}, Invitrogen) antibiotics. They were trypsinized (2 mL, Invitrogen) to form a monolayer culture and seeded at cell densities of ~10^6 cells mL^{-1}. RAW macrophages that contain H2B-DsRed nuclear marker and p65-GFP[24] were cultured in a

DMEM with FBS (10%), GlutaMax (1×) and HEPES (2 mM, Invitrogen). Cells were harvested by using Versene (5 mL, Invitrogen) and loaded at $\sim 10^6$ cells mL^{-1}.

Imaging and experimental set-up

The cells were tracked in the device using an automated Leica DMI6000B microscope (10× air objective, NA = 0.3) and the H2B:GFP/DsRed nuclear markers. The total time for imaging the entire chip (30 chambers) with two fluorescent and one brightfield images takes 95 s. The microscope was enclosed in a cell culture box that maintains a constant temperature of 37 °C and 5% CO_2. The PDMS chip was further enclosed in a transparent box maintaining an additionally humid environment of 60% in order to provide an iso-osmotic condition in the chip preventing evaporation of water through PDMS.

NFκB signalling quantification

NFκB nuclear localization in single-cells was performed using a custom-made tracking algorithm coded in MATLAB as reported in ref. 14. Briefly, a *k*-means clustering algorithm detects the nuclei of cells using the GFP marker, and then the nuclear intensities are measured. Cells were further checked and corrected for small size, overlapping cells and the background.

Finite-element simulation

All finite element (FEM) simulations were done in COMSOL Multiphysics (v4.2a). The device was simulated then by using the creeping flow physics as well as the diluted species physics. For the flow properties the density of water (1000 kg m^{-3}) and the dynamic viscosity of 1 mPa s was used. A diffusion coefficient of D = 100 μm^2 s^{-1} was used to model the typical protein. Flow was created by having the inlets set to 0.1 bar and outlets to 0 bar. The basic physics of the simulation is based on solving the Navier–Stokes equation and using Ficks' Law. For the concentration profile of the gradient a first-order photo bleaching reaction was included with a measured half-life of $t_{0.5}$ = 7.5 min.

Results and discussion

Basic chamber geometry and gradients

The design of the final device was based on a single chamber element shown in Fig. 1B that can be scaled to a multichamber device (Fig. 2A). As discussed earlier, a gradient is easily created by diffusion of proteins from high to low concentrations if the source and sink are maintained at constant concentration. This geometry was established here by using two support channels (width w = 100 μm and height h = 40 μm) that allows flow by a pressure difference between inlet and outlet, that leads to a working sink or source respectively. A flow-free diffusion area (l = 1000 μm, w = 250 μm and h = 100 μm) for cell culture was placed between the supply channels. Since the flow lines will go into the chambers at the edges (Supp. Fig. 3†), a buffer space of 300 × 250 μm^2 was implemented in order to have the actual cell chamber of 1 mm be absolutely diffusion dominated (Pe < 1).

In order to avoid flow through the chamber by a pressure difference between the two supporting channels (Supp. Fig. 1†), valves were placed at the inlet and outlet (Fig. 1D). Since diffusion of proteins is rather slow (D = 100 μm^2 s^{-1}) and advection is very fast, we switched between flow and no flow in order to create and maintain the gradient without creating a pressure difference between the two supply channels. We found that a maintenance cycle below 5 min should obtain a gradient with maximal 10% relative variation (Supplementary Fig. 6†). Flow at 5 mm s^{-1} results in eliminating advection dominated areas in the diffusion (cell culture) region, and provides total replacement of the support channels within less then a second. In order to test this experimentally, a gradient was established by using FITC–Dextran (M = 40 kDa, c_0 = 300 μM) in PBS by flowing the source channel for 1 s. After 59 s of no flow, PBS sink was flowed for 1 s, which was preceded by a no flow condition for 59 s before the next cycle was started again (Fig. 1C and Supp. Fig. 4†). This resulted in a total maintenance cycle time of 2 min. This way, a stable gradient was formed after 80 min in the diffusion chamber (Fig. 1E–G). Also an opposing, two-sided, robust gradient was possible by using Rhodamin–Dextran (M = 40 kDa, c_0 = 50 μM) in the sink channel. The flow-switching with a 2 min maintenance cycle creates negligible fluctuation across the diffusion chamber and results in extremely stable concentration profiles, with less than 5% variation in 17 h at any given location in the chamber (Fig. 1G). The steady state gradient profile is dependent on the length of the chamber, the diffusion coefficient, the decay rate and the concentrations of the sink and the source (see the ESI†). Since the device geometry, diffusion coefficient and the decay rate are constant, the gradient shape can be controlled by the concentrations of the source and the sink.

Multi-chamber device for high-throughput cell culture in chemical gradients

The single unit discussed above has a maintenance cycle time of two minutes. Within these two minutes, we have 158 s where no flow needs to be applied, while still maintaining the gradient. To take advantage of this waiting time, we fabricated a device with several parallel chambers (Fig. 2A). The two supply channels were then periodically filled with different media compositions using the media input manifold, and each diffusion chamber was exposed to these conditions for only one second every two minutes. The number of chambers is limited to the maintenance cycle and the channel clearing time. Due to the rectangular geometry at the edges there are small areas with almost no flow and therefore a long washing process needs to be applied. A FEM simulation showed that 5 s of flow should maintain a full replacement of the channels, supporting a total of 10 chambers in series without cross-contamination. An arbitrary number of such serial chambers rows can be integrated in parallel units to create replicates. We placed three such elements in parallel, resulting in a total of 30 experiments with 10 different conditions and 3 replicates possible at once (Fig. 2A). This series device was then tested for its capability to create different gradient conditions. Different food dye mixtures were used to show that 30 stable gradients could be obtained and maintained in parallel (Fig. 2B and C).

The variation between the replicates was found to be extremely small (Fig. 2C), creating almost identical replicates along the columns of the device.

Automation

We implemented a custom LabVIEW program, that allows the experimenter to control the valves either manually or through predefined programs that execute certain modes like PDMS coating, cells seeding, gradient generation, imaging and cleaning. Supplementary Fig. 5† describes experimental protocol and automated steps for 3T3-Fibroblast measurements. The chip is first flushed and rinsed with Phosphate Buffer Saline (PBS). Afterwards, the cell culture (diffusion) chambers are sealed by closing the inlet valves. Pluronic, which prevents cell attachment, is flushed through the supply channels and incubated for 5 min. The channels are then washed for 10 min in order to remove all non-coated Pluronic. Then each chamber is flushed with Fibronectin for 10 min and incubated for 10 h. Instead of Fibronectin the procedure can be modified for different coating materials. The cells are seeded in several cycles. We found that after 3 min, all 3T3 cells in a solution ($\sim 10^6$ cells mL^{-1}) attach to the Fibronectin coated PDMS chamber. Higher cell densities can be achieved by using multiple seeding cycles. Coupled with an automated microscope, this device allows many experiments in parallel to increase the throughput of cell-biological measurements.

Multi-parameter single-cell analysis of NFκB signalling in chemical gradients

In order to test the ability of the device for single-cell analysis in cell signalling applications, we cultured 3T3 fibroblast, RAW macrophages and primary human T-cells in the 30-plex device, and exposed them to various gradients that signal through the NFκB pathway (Fig. 3 and 4). NFκB is an innate immune regulator that detects pathogen-derived signals or secreted signalling molecules, which in turn regulates the expression of thousands of response genes. Due to its importance in basic biological functions and disease (autoimmunity, infection and cancer), NFκB has been a major field of research in cell signalling.[14,25] We performed multi-parameter analysis of this pathway in single-cells, quantifying various cellular traits including adhesion, migration and responses to gradients of inflammatory signalling molecules. In total $N = 1475$ cells were analyzed in gradients of LPS, TNFα, PDGF-BB, and regular cell culture medium as a negative control.

NFκB is a dimeric protein that is bound to IκB in the cytosol in unstimulated cells. Upon an external stimulus (*e.g.* LPS), IKK kinase gets activated and phosphorylates IκB, leading NFκB to be transported to the nucleus where it acts as a transcription factor of a number of genes. One of these genes is IκB, and newly synthesized IκB protein leads to a negative feedback by capturing NFκB and moving it out of the nucleus (Fig. 3A).[14,25] This activation and nuclear shuttling can be observed by using a fluorescent marker fused to NFκB-subunit p65, as shown in Fig. 3 and 4. The control experiment where the cells were cultured in plain DMEM medium showed no NFκB activation. The viability in this culture was 107% within 12 h, *i.e.* the cells survived and proliferated.

3T3 fibroblasts in gradients of LPS, PDGF and TNFα

The 3T3 fibroblasts were seeded at a high cell density ($\sim 10^6$ cells mL^{-1}) and as a result, long-range migration was mostly inhibited by contact inhibition. The chambers were analyzed into three concentration ranges, namely high concentration range, middle concentration range and low concentration range (Fig. 3C–E). The multi-parameter analysis showed spatiotemporally dependent signalling in the gradients. The LPS experiment (Fig. 3C) showed a first peak in all regions in the gradient due to primary LPS stimulation (Supplementary Movie 1†). As expected, the mean time of the first peak is dependent on the position of the cells in chamber. At high concentration locations the signalling onset is earlier than in low concentration because the gradient is still building up, and higher concentrations lead to faster response times[14] (Fig. 3C). At high concentration locations, the cells showed a second peak after roughly 200 min. We have not previously observed such an LPS induced secondary peak in experiments with spatially homogenous cultures. In the middle range, there are several peaks observed within 10 h, this time is in agreement with experiments under spatially homogenous LPS stimulation. In the low range there is a main peak, and some cells showed a secondary weaker peak. The late secondary peaks can be explained by a paracrine TNFα signal that is upregulated in cells that are stimulated with LPS,[26] which then can build up secondary gradients. This paracrine secondary peak would not have been seen if flow was applied, since secreted TNFα molecules would be washed away.

Compared to LPS, the high-dose growth factor PDGF-BB shows one main peak (Fig. 3D and Supplementary Movie 2†). The response time of the main peak is location dependent, and is delayed by roughly 30 min with respect to LPS induced peaks. PDGF acts through Rac/PI3K signalling to NFκB – an indirect activation mechanism – that explains this observed delay.[27] PDGF was reported to stimulate fibroblast proliferation.[27] In the gradient we see that the highest proliferation rate was seen in the middle concentration range. A second NFκB peak is only seen if proliferation starts (a by-product of nuclear membrane breakdown during mitosis). The absence of a second peak in non-dividing cells suggests that no downstream product is secreted.

TNFα stimulation led to a main peak at high and middle concentration ranges in many cells, but fewer cells activated at low dose locations in the gradient (Fig. 3E). This behaviour is in agreement with the digital activation of NFκB under TNFα.[14] Uncharacteristically for TNFα, some cells showed long-term activation, but second peaks are not seen. The lack of late-term secondary peaks is expected, as the amount of TNFα secreted upon TNFα stimulation is very low in fibroblast cells. The onset of activation is delayed in the low dose range, similar to that seen under LPS.

RAW macrophages in LPS gradient

In fibroblasts LPS showed a dose-dependent population wide response. In LPS stimulated RAW macrophages the behaviour at early time points was similar, with all cells activating NFκB, with delayed response time at lower dose locations (Fig. 4). A major difference is the lack of LPS induced NFκB oscillations

in the middle range (Fig. 4E). Nevertheless, some cells showed a second peak at about 430 min (possibly due to secreted TNFα), but most of the cells remained in an inactive state after the first LPS induced peak. This can be explained by our previous observations showing that the threshold of TNFα activation is very high, above 10 ng mL^{-1}, for RAW macrophages. The cell density was lower than in the 3T3 experiment, and thus some cells exhibited motile behaviour, moving away from the LPS source as seen in Fig. 4C and D. We traced these cells and showed that the migration is predominantly along the gradient axis (Fig. 4D). Fig. 4E shows the NFκB nuclear profiles as the cells move away from the LPS source, demonstrating the usefulness of our system in analyzing spatiotemporal characteristics of cell signalling under chemical gradients.

Conclusions

By using a new technique based on temporal modulation of flow, we were able to implement a robust gradient generator for long-term cell signalling studies. The strength of the diffusion chamber design lies in its simplicity, which translates into a capability to parallelize experiments and create complex, independently programmable gradients. Membrane valves and automation enhance these advantages by reducing man-made errors and providing efficient use resources. We demonstrated a total-analysis system that can generate 30 independent diffusion-based gradients side-by-side, with 10 different chemical compositions and 3 replicates. These gradients were extremely stable for weeks, with minimal change of the protein concentration at a given location. The chip creates flow-free conditions for cells, allowing the use of a variety of adhering and non-adhering cells including fibroblasts, macrophages, T-cells, yeast and bacteria. The lack of flow allows cells to communicate with each other through secreted signalling molecules such as TNFα. The microfluidic chip can be extended to even higher throughputs due to its geometric simplicity.

We screened mouse fibroblasts and macrophages under different chemical conditions at once, and confirmed experiments about digital TNFα and LPS induced NFκB activity in single-cells. We observed uncharacteristic late term NFκB activity that can be attributed to paracrine signalling, demonstrating the utility of diffusion-based gradient systems. The system generates extremely stable gradients of any soluble protein, and maintains parallel experiments in the 30-plex chip. Long-term, temporally changing gradients can easily be implemented. The system can further be improved by using a microfluidic mixer on the chip to create even more complex concentration mixtures, and its throughput can be improved an order of magnitude within the limits of standard multilayer soft lithography. Such a system can be applied to various problems in developmental biology, tissue engineering, and cell signalling. Compact, field-deployable systems can be realized by combining our chip with lens-free, computational on-chip microscopy techniques.[28] The versatile cell culture device shown here can start a new generation of gradient generators allowing defining precise chemical conditions, parallelized screens, and long-term gradients for systems biology studies.

Acknowledgements

This work was funded by ETH Zurich and Swiss National Science Foundation grant 205321-141299. The authors thank Dagmar Iber and Simon Tanaka for useful discussions, and Stanford Microfluidics Foundry for support with chip fabrication.

Notes and references

1 A. D. Lander, *Cell*, 2007, **128**, 245–256.
2 U. H. von Andrian and T. R. Mempel, *Nat. Rev. Immunol.*, 2003, **3**, 867–878.
3 W. Driever and C. Nüsslein-Volhaard, *Cell*, 1988, **54**, 95–104.
4 M. Tessier-Lavigne and C. S. Goodma, *Science*, 1996, **274**, 1123–1133.
5 C. L. Jackson and L. H. Hartwell, *Cell*, 1990, **63**, 1039–1051.
6 D. Irmia, D. A. Geba and M. Toner, *Anal. Chem.*, 2006, **78**, 3472–3477.
7 N. L. Jeon, S. K. W. Dertiger, D. T. Chiu, I. S. Choi, A. D. Stroock and G. M. Whitesides, *Langmuir*, 2000, **16**, 8311–8316.
8 K. Sudong, J. K. Hyung and N. L. Jeon, *Integr. Biol.*, 2010, **2**, 584–603.
9 M. Morel, J. C. Galas, M. Dahan and V. Studer, *Lab Chip*, 2012, **12**, 1340–1346.
10 H. Yin, Z. Zhang, N. Pattrick, N. Klauke, H. C. Cordingley, S. J. Haswell and J. M. Cooper, *Anal. Chem.*, 2007, **79**, 7139–7144.
11 F. Moledina, G. Clare, A. Oskooei, K. Onishi, A. Günther and P. W. Zandstra, *Proc. Natl. Acad. Sci. U. S. A.*, 2012, **109**, 3264–3269.
12 G. M. Walker, J. Sai, A. Richmond, M. Stremier, C. Y. Chung and J. P. Wikswo, *Lab Chip*, 2005, **5**, 611–618.
13 R. Cheong, A. Bergmann, S. L. Werner, J. Regal, A. Hoffmann and A. Levchenko, *J. Biol. Chem.*, 2006, **281**, 2945–2950.
14 S. Tay, J. J. Hughey, T. K. Lee, T. Lipniacki, S. R. Quake and M. W. Covert, *Nature*, 2010, **466**, 267–272.
15 S. S. Lee, P. Horvarth, S. Pelet, B. Hegemann, L. P. Lee and M. Peter, *Integr. Biol.*, 2012, **4**, 381–390.
16 T. M. Keenan, C.-H. Hsu and A. Folch, *Appl. Phys. Lett.*, 2006, **89**, 114103.
17 S. Paliwal, P. A. Iglesias, K. Campbell, Z. Hilioti, A. Groisman and A. Levchenko, *Nature*, 2007, **446**, 46–51.
18 B. Mosadegh, C. Huang, J. W. Park, H. S. Shin, B. G. Chung, S. K. Hwang, K. H. Lee, H. J. Kim, J. Brody and N. L. Jeon, *Langmuir*, 2007, **23**, 10910–10912.
19 U. Haessler, M. Pisano, M. Wu and M. A. Swartz, *Proc. Natl. Acad. Sci. USA*, 2011, **10**, 1073.
20 J. J. VanDersarl, A. M. Xu and N. A. Melosh, *Lab Chip*, 2011, **11**, 3057–3063.

21 T. Thorsen, S. J. Maerkl and S. R. Quake, *Science*, 2002, **298**, 580–584.
22 M. A. Unger, H. P. Chou, T. Thorsen, A. Scherer and S. R. Quake, *Science*, 2000, **288**, 113–116.
23 https://sites.google.com/a/lbl.gov/microfluidics-lab/valve-controllers/usb-based-controller.
24 E. A. Wall, J. R. Zavzavadjian, M. S. Chang, B. Randhawa, X. Zhu, R. C. Hsueh, J. Liu, A. Driver, X. R. Bao, P. C. Sternweis, M. I. Simon and I. D. Fraser, *Sci. Signaling*, 2009, **2**(75), ra28.
25 A. Hoffman and D. Baltimore, *Immunol. Rev.*, 2006, **210**, 171–186.
26 M. W. Covert, T. H. Leung, J. E. Gaston and D. Baltimore, *Science*, 2005, **309**, 1854–1857.
27 J. A. Romashkova and S. S. Makarov, *Nature*, 1999, **401**, 86–90.
28 W. Bishara, U. Sikora, O. Mundanyali, T.-W. Su, O. Yaglidere, S. Luckhart and A. Ozcan, *Lab Chip*, 2011, **11**, 1276.